

Two Efficient Approaches for Improving Field Emission Properties of ZnO NRs

Marziyeh Advand^{1,2}, Bahram Azizolah Ganji^{*1}, Mohammadreza Kolahdouz²

1- Department of Electrical and Computer Engineering, Babol Noshirvani University of Technology, Babol, Iran

Email: baganji@nit.ac.ir (Corresponding author)

2- Department of Electrical and Computer Engineering University of Tehran, Tehran, Iran

Email: marziyeh.advand@gmail.com

Received: January 2017

Revised: January 2017

Accepted: January 2017

ABSTRACT:

The structure of pure and Al doped ZnO (AZO) nanorods (NRs) has been studied. A post annealing procedure in oxygen ambience at 400C were used in order to improve crystallinity of both group of samples. The XRD patterns illustrate that the Al doped ZnO NRs were successfully synthesized using our method. Then, the field emission properties of the as grown NRs before and after annealing process were evaluated by our home-made setup. Experimental results show that Al density in ZnO NRs directly affects FE properties of these samples. The oxygen post annealing process leads to a significant improvement in the field emission performances of pristine and doped ZnO NRs including considerably lower turn on voltage, and higher emission current.

KEYWORDS: Zinc oxide, Al-doped Zinc Oxide, Nanorods, Field Emission, Oxygen Annealing, Oxygen Vacancy

1. INTRODUCTION

Field emission effect plays an important role in high sensitivity gas and pressure sensing[1], flat panel displays[2], [3] and telecommunication devices such as compact microwave amplifiers[4]. In this manner, the understanding of the field emission that occurs in the electronic and communication devices like RF-MEMS switches is a very important issue[5], [6]. Exponential relationship between voltage and current in field emission mechanism results in high-precision measurements[7]. Therefore, it can be used for high accuracy detection of low concentrations gases. The use of field emission method is more attractive for gas sensing because of high-speed amenability and its low power consumption[8]. Turn-on field (E_{to}), threshold field (E_{th}), emission current density, field screening effect and field enhancement factor (β) are the main factors that determine field emission performance of materials[9]. In this manner, ZnO is a promising candidate for the acutely effective cathode emitters due to its chemical stability and its high device packaging density[10]. In order to achieve an excellent FE performance from ZnO NRs array, the array's resistance, work function through the energy band binding and the quality of metal contact are important[11]. Therefore, ZnO doping with Aluminum and a post annealing procedure in oxygen ambience can positively affect the FE properties of ZnO nanostructures[12]. This method adjusts internal

bandgap of nanostructure and its carrier concentration[12].

In this paper, the morphology of the as grown ZnO arrays were investigated using top view and cross-sectional view FESEM images. The crystalline quality of all the samples was investigated using X-ray diffraction method. Finally, the IV curves and field emission responses were measured by Keithley-K361 parameter analyzer in a vacuum chamber (~ 1.33 Pa) at room temperature to determine the effect of doping process and oxygen annealing on the enhancement of Fermi level and reduction of the work function.

2. MATERIALS AND METHODS

In order to investigate the ZnO NRs' field emission properties, different percentages of Al were doped into ZnO NRs. For this purpose, $6 \times 6 \text{ mm}^2$ glass substrates were purified by sonicating in acetone, ethanol, and de-ionized (DI) water. The glass substrates were utilized for strong insulating and the growth of Al-doped NRs. Then, 250 nm layer of titanium and 350 nm-thick layer of gold were consecutively deposited on the purified glass substrate by radio frequency (RF) plasma sputtering. The titanium thin film layer was used as an adhesive layer to improve interfacial bonding between the glass substrate and the gold thin film. After that, 200nm thickness of 2% Aluminum-doped ZnO (AZO) seed layer was deposited on the Au layer by RF sputtering system (Fig.1). In the next step,

in order to grow the ZnO NRs using chemical bath deposition, the sample was suspended face down in the nutrient solution. The nutrient solution (100ml) made up of an equimolar (1:1) of zinc nitrate hexahydrate powder ($\text{Zn}(\text{NO}_3)_2 \cdot 6\text{H}_2\text{O}$, Merck, Germany) and hexamethylenetetramine powder (HMTA, $\text{C}_6\text{H}_{12}\text{N}_4$, Merck, Germany). The doping precursor, aluminum nitrate nonahydrate powder ($\text{Al}(\text{NO}_3)_3 \cdot 9\text{H}_2\text{O}$, Merck, Germany), was added to the solution by varying the atomic ratio of Al to Zn between 1 to 4%. The process lasted 6 hours at 90°C . After the growth, ZnO NRs were formed vertically on the substrate with an average height of $2.9(\pm 0.2) \mu\text{m}$. A post annealing procedure in oxygen ambience at 400°C for 20 minutes was used in order to improve crystallinity of both group of samples. The morphology of the as grown NRs was monitored using field emission scanning electron microscope (FESEM, HITACHI S-4160). In addition, X-ray diffraction (XRD) by Philips Xpert, with Cu-K α radiation ($\lambda=0.15418 \text{ nm}$) was performed to explore the effects of doping concentration on the crystallinity of ZnO NRs. The as-synthesized products were also characterized by transmission electron microscopy (TEM, JEM-2010-JEOL, Japan, 400 kV). The field emission studies were carried out in a chamber in a vacuum of $\sim 1.33 \text{ Pa}$ at room temperature. The annealing step was executed in a tube furnace with oxygen gas flow rate of 70 sccm at the pressure of $\sim 1 \text{ bar}$, annealing temperature of 400°C , and 1 h duration. The cathode was the as grown pure ZnO NRs and the oxygen annealed ZnO NRs. Metal anode with diameter of 6 mm was then placed on top of the sample surface. For the field emission measurement, the separation between the anode and the cathode was fixed at $120 \mu\text{m}$. After evacuating the chamber, an external voltage with ascending magnitude is applied to the anode and the resulting emission current was measured using a Keithley-K361 parameter analyzer. The testing electric field (E) was estimated by dividing the applied voltage (V) by the anode-cathode distance (V/d). The emission current density (J) was calculated from the obtained emission current. The emission current-voltage characteristics were analyzed by using the Fowler-Nordheim (FN) equation.



Fig. 1. Schematic diagram of AZO/Au deposition on the glass substrate for manufacturing electrode

3. RESULT AND DISCUSSIONS

This study show the effect of doping and post annealing process on the FE behavior of ZnO NRs. The experiments were performed by changing the

percentage of Al element in ZnO NRs and post annealing procedure in oxygen ambience at different temperatures.

3.1. Structure and morphology

Pure ZnO NRs have undeviating shapes and similar diameters as indicated in TEM image of a generic ZnO NR (Fig.2).

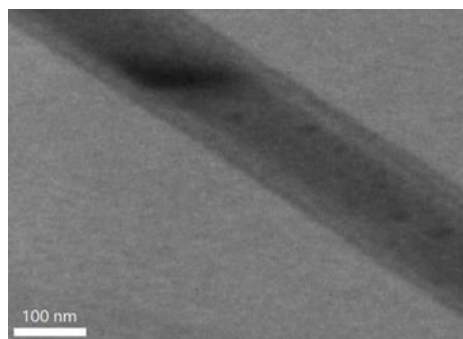


Fig. 2. TEM image of a typical ZnO NR

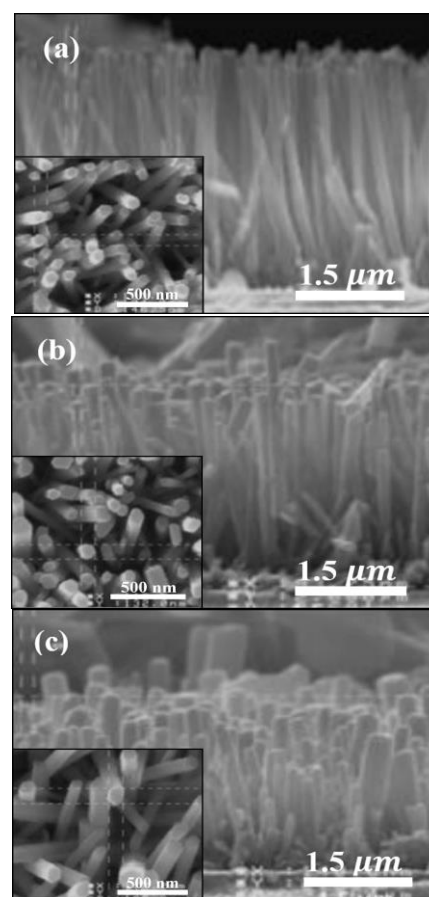


Fig. 3. Top view and cross-sectional view SEM images of ZnO nanostructures with (a) 1% Al; (b) 3% Al; (c) 4% Al.

As illustrated in Fig.3. the remarkable changes were occurred in the morphology of the Al doped ZnO materials, because increasing Al percentage in ZnO NRs from 1 to 4% causes an increase in the diameters of the nanostructures.

As shown in Fig.3. (d), doping of ZnO NRs with 6% Al notably disturbed the vertical growth of NRs along the c-axis normal to the substrate and converted them into the ZnO nano plates.

It can be seen in Fig. 3 that the polar orientation growth (c-axis) was changed and the average diameters were rose up in the high concentration Al (OH)₄ sample. Fig. 4. Illustrates that the XRD curves of pure ZnO NRs and Al-doped ZnO NRs doped with 1% Al; 3% Al; 4% Al. This figure indicates that the single-crystal NRs have successfully grown at the low temperature (85-90 ° C). Furthermore, X-ray diffraction peaks of Al-doped samples do not show significant changes in location relative to pure ZnO NRs. This means that the lattice parameters of doped samples have not changed and they have the same wurtzite structure and no trace of aluminum nitrate or its composites can be detected in these results[13].

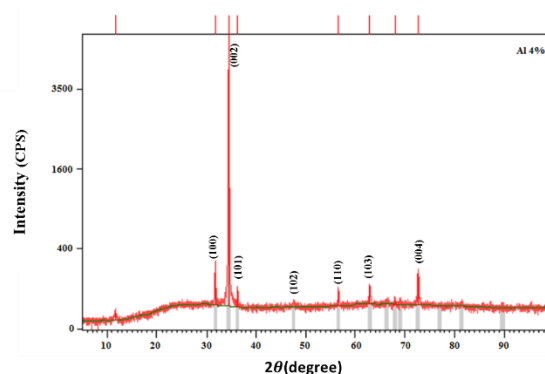
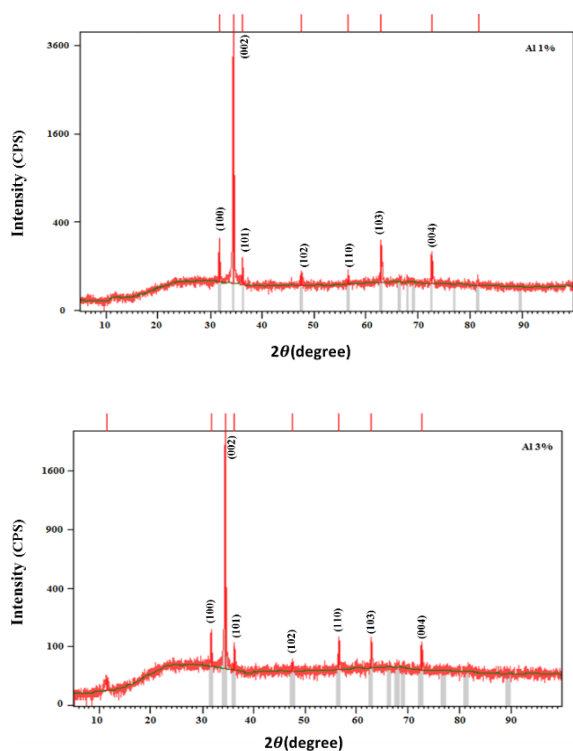


Fig. 4. The X-ray diffraction spectra of ZnO NRs with different percentage of Al doping

3.2. Field emission characteristics

It was established that the emission effect occurs from small regions called emission centers. The size of these emission centers are about 4–5 nm and their numbers and arrangements can vary widely[14]. The emission maxima clearly corresponds to the morphology pits (grain boundaries). These emission centers are often associated to regions with reduced value of work function which occurred on top of the grains.

The schematic diagram of our field emission measurement setup is shown in Fig. 5. The experiment was accomplished by applying a negative voltage to the Au thin film with respect to the anode plate. Anode is a parallel plate on top of the sample and can move accurately by a micrometric mechanical stage. Effective area in the field emission measurement was about 0.3 cm² while the anode–cathode spacing was fixed at about 250μm. After evacuating the chamber, an external voltage with ascending magnitude is applied to the anode and the resulted emission current was measured using a Keithley-K361 parameter analyzer.

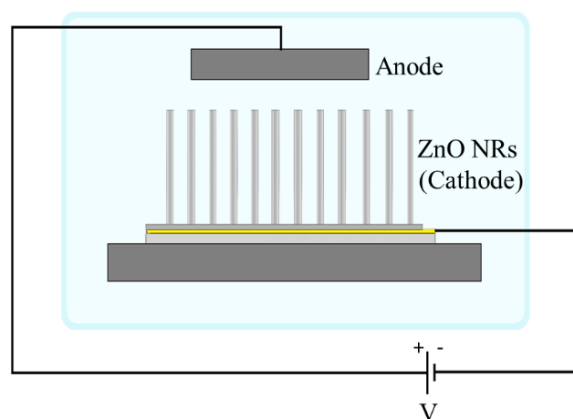


Fig. 5. The schematic of the setup used for the field emission investigation. The sample is fixed on the bottom plate and connected to the negative voltage source. The anode is a movable plate on top of the sample, with a positive bias voltage.

The current density versus applied field (J-E) curves of Al doped and pure ZnO NRs before and after oxygen annealing are demonstrated in Fig. 6. As it can be seen, the field emission properties improve due to the oxygen annealing. This effect is mainly attributed to the fact that oxygen annealing improves the crystal structure of ZnO NRs and compensates the structural defects of them[15]. Furthermore, the field emission current of the NRs is increased with the Al-doping of the NRs because of the fact that Fermi level shifts up with the increased Al doping concentration in ZnO NRs which results in reduction of the work function. In consequence, the turn-on field (E_{t_o}) and the threshold field (E_{t_h}) are lowered with the increasing doping concentration. E_{t_o} and E_{t_h} are specified as the macroscopic fields required to produce a current density of 1 $\mu\text{A}/\text{cm}^2$ and 1 mA/cm^2 , respectively. The variation of field emission properties in NRs can be explained easily by the classic Fowler–Nordheim (F–N) law[16],[17]:

$$\ln\left(\frac{I}{V^2}\right) = \ln A - \frac{B}{V} \quad (1)$$

$$A = 1.54 \times 10^{-6} n_a \frac{\beta^2}{\varphi}, B = \frac{-6.83 \times 10^7 \varphi^{\frac{3}{2}} d}{\beta} \quad (2)$$

Where β is the field enhancement factor, I is the emission current, V is the applied voltage, φ is the work function of the emitters, n_a (cm^2) is the emission area and d (cm) is the distance between the electrodes. The linearity of this plot indicates the exponential field emission behavior.

According to the F–N theory, the emission current is governed by the work function of the material, the applied field and the field enhancement factor. In order to describe the emitted current (J) of a single emitter over a wide range of the local field at the emitter surface (E) as follows[17]:

$$E_{Local} = \beta E = \beta \frac{V}{d} \quad (3)$$

Where d is the inter-electrode distance, V is the applied voltage and β (the field enhancement factor) quantifies the ability of the emitter to amplify the E . We have used the following simplified F–N formula proposed by Gadzuk and Plummer[18]:

$$I = A \frac{E_{Local}^2 \beta^2}{\varphi} \exp\left(-\frac{B \varphi^{1.5}}{E_{Local}}\right) \quad (4)$$

Where φ is the work function for electron emission, A and B are defined constants ($A = 1.56 \times 10^{-10} (\text{AV}^{-2}\text{eV})$ and $B = 6.83 \times 10^3 (\text{V eV}^{-3/2} \mu\text{m}^{-1})$) and β is introduced to reveal the degree of the field

emission enhancement of any tip over a flat surface[19]. The logarithmic equivalent of Eq. (4) is called a Fowler–Nordheim (FN) plot. The linearity of this plot indicates the exponential field emission behavior.

The field enhancement factor can be calculated from the slope of the F–N plots, assuming the work function of ZnO is 5.3 eV[20]. Based on fig. 6, the field enhancement factor β were estimated to be 761, 840 and 951 for the ZnO NRs doped with 1% Al, 3% Al, 4% Al, respectively before their annealing process. It can be estimated from fig. 6 that the turn on field for the samples before annealing decreases in as 0.946, 0.88 and 0.7 $\text{V}/\mu\text{m}$ with increasing the Al-doping of the NRs. After oxygen annealing process, the field enhancement factor β were changed to 861, 973 and 968 for the samples with 1% Al, 3% Al, 4% Al, respectively. Hence, the estimated high β and low turn-on field indicate that the oxygen annealed Al-doped ZnO NRs are excellent field emitters. As it is shown in magnified region of fig. 6, field enhancement factor and turn-on field are not allocated to pure ZnO NRs due to their low field emission current.

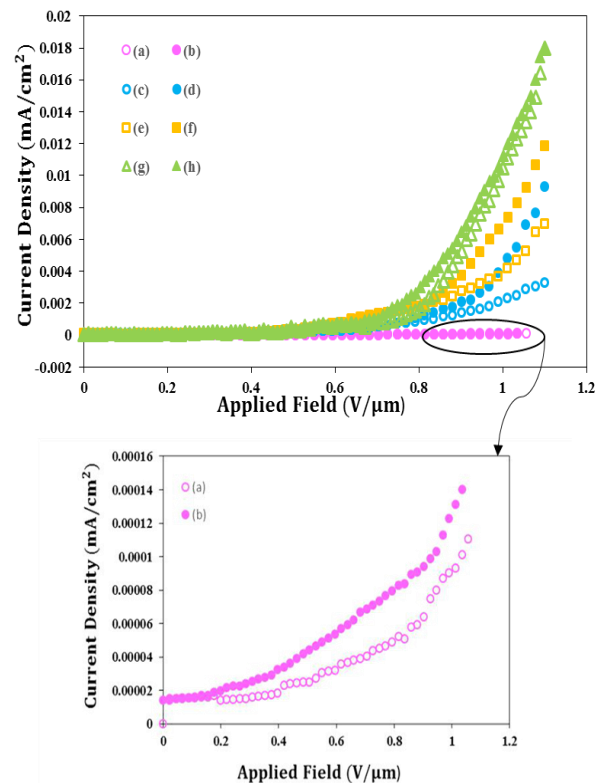


Fig. 6. Field electron emission properties of (a) pure ZnO (b) pure ZnO after O_2 annealing and Al-doped ZnO nanorods deposited at (c) 1 wt.%, (d) 1 wt.% after O_2 annealing, (e) 3 wt.%, (f) 3 wt.% after O_2 annealing. (g) 4 wt.%, (h) 4 wt.% after O_2 annealing.

Table 1. The effect of the Al doping concentration and oxygen annealing on Field emission properties of ZnO NRs

Samples	0 wt%	1 wt%	3 wt%	4 wt%
E_{t_0} (V/ μ m) (before annealing)	-----	0.902	0.726	0.692
E_{t_0} (V/ μ m) (after annealing)	-----	0.792	0.638	0.612
Mean diameter 2r (nm)	94	98	114	137
Mean height h (μ m)	2.8	2.2	2.59	2.3
ϕ	5.3	4.11	4.06	3.96
β (before annealing)	-----	772	850	962.7
β (after annealing)	-----	861	973	968

4. CONCLUSION

In summary, we synthesized Al doped ZnO NRs and characterized their field emission properties. In addition, we studied the effect of post annealing process on the field emission characteristics of pure and doped ZnO NRs. Our results suggests that the field emission properties improve with the increased Al doping concentration in ZnO NRs. The field enhancement factor β is enhanced by ~25 % through 4 wt% Al doping. The field emission properties can be further improved by annealing in oxygen environment. Oxygen annealing modified the crystal structure of ZnO NRs and improves their field emission properties. Therefore, the 4 wt% Al doped sample with oxygen post annealing demonstrates the best field emission performance.

REFERENCES

- [1] N. Doostani, S. Darbari, S. Mohajerzadeh, and M. K. Moravvej-Farshi, "Fabrication of highly sensitive field emission based pressure sensor, using CNTs grown on micro-machined substrate," *Sensors Actuators A Phys.*, vol. 201, pp. 310–315, Oct. 2013.
- [2] W. B. Choi *et al.*, "Fully sealed, high-brightness carbon-nanotube field-emission display," *Appl. Phys. Lett.*, Vol. 75, No. 20, pp. 3129–3131, Nov. 1999.
- [3] Y. Abdi, J. Koohshorkhi, S. Mohajerzadeh, S. Darbari, and Z. Sanaee, "Embedded vertically grown carbon nanotubes for field emission applications," *J. Vac. Sci. Technol. B Microelectron. Nanom. Struct.*, Vol. 25, No. 3, p. 822, 2007.
- [4] K. B. K. Teo *et al.*, "Microwave devices: Carbon nanotubes as cold cathodes," *Nature*, Vol. 437, No. 7061, pp. 968–968, Oct. 2005.
- [5] J. Ruan *et al.*, "ESD failure signature in capacitive RF MEMS switches," *Microelectron. Reliab.*, Vol. 48, No. 8–9, pp. 1237–1240, Aug. 2008.
- [6] L. Michalas *et al.*, "A study of field emission process in electrostatically actuated MEMS switches," *Microelectron. Reliab.*, Vol. 52, No. 9–10, pp. 2267–2271, Sep. 2012.
- [7] K. P. Ghatak, S. Bhattacharya, A. Mondal, S. Debbarma, P. Ghorai, and A. Bhattacharjee, "On the Fowler-Nordheim Field Emission from Quantum-Confined Optoelectronic Materials in the Presence of Light Waves," *Quantum Matter*, Vol. 2, No. 1, pp. 25–41, Feb. 2013.
- [8] L. Li, K. Yu, Y. Wang, and Z. Zhu, "Photoluminescence and field emission properties of Sn-doped ZnO microrods," *Appl. Surf. Sci.*, Vol. 256, No. 11, pp. 3361–3364, Mar. 2010.
- [9] D. Sarkar, C. K. Ghosh, and K. K. Chattopadhyay, "Morphology control of rutile TiO₂ hierarchical architectures and their excellent field emission properties," *CrystEngComm*, Vol. 14, No. 8, p. 2683, 2012.
- [10] L. Liao, J. C. Li, D. F. Wang, C. Liu, and Q. Fu, "Electron field emission studies on ZnO nanowires," *Mater. Lett.*, Vol. 59, No. 19–20, pp. 2465–2467, Aug. 2005.
- [11] Xiaomeng Song *et al.*, "Comparative study of field emission from individual ZnO nanowire with and without NH₃ plasma treatment," in *2015 28th International Vacuum Nanoelectronics Conference (IVNC)*, 2015, pp. 150–151.
- [12] J.-L. Wang, T.-Y. Hsieh, P.-Y. Yang, C.-C. Hwang, D.-C. Shye, and I.-C. Lee, "Oxygen annealing effect on field-emission characteristics of hydrothermally synthesized Al-doped ZnO nanowires," *Surf. Coatings Technol.*, Vol. 231, pp. 423–427, Sep. 2013.
- [13] R. Zou, G. He, K. Xu, Q. Liu, Z. Zhang, and J. Hu, "ZnO nanorods on reduced graphene sheets with excellent field emission, gas sensor and photocatalytic properties," *J. Mater. Chem. A*, Vol. 1, No. 29, p. 8445, 2013.
- [14] F. Dehghan Nayeri, K. Narimani, M. Kolahdouz, E. Asl-Soleimani, and F. Salehi, "Surface structure optimization for cost effective field emission of zinc oxide nanorods on glass substrate," *Thin Solid Films*, Vol. 571, pp. 154–160, Nov. 2014.
- [15] S. Chen, J. Chen, J. Liu, J. Qi, and Y. Wang, "The effect of high-temperature oxygen annealing on field emission from ZnO

- nanowire arrays,” *Appl. Surf. Sci.*, Vol. 357, pp. 413–416, Dec. 2015.
- [16] J. Song *et al.*, “**Epitaxial ZnO Nanowire-on-Nanoplate Structures as Efficient and Transferable Field Emitters**,” *Adv. Mater.*, Vol. 25, No. 40, pp. 5750–5755, Oct. 2013.
- [17] R. H. Fowler and L. Nordheim, “**Electron Emission in Intense Electric Fields**,” *Proc. R. Soc. A Math. Phys. Eng. Sci.*, Vol. 119, No. 781, pp. 173–181, May 1928.
- [18] J. W. Gadzuk and E. W. Plummer, “**Field Emission Energy Distribution (FEED)**,” *Rev. Mod. Phys.*, Vol. 45, No. 3, pp. 487–548, Jul. 1973.
- [19] C. Li *et al.*, “**Enhanced field emission from injector-like ZnO nanostructures with minimized screening effect**,” *Nanotechnology*, Vol. 18, No. 13, p. 135604, Apr. 2007.
- [20] K.-S. Park *et al.*, “**Enhancement of Field-Emission Properties in ZnO Nanowire Array by Post-Annealing in H₂ Ambient**,” *J. Nanosci. Nanotechnol.*, Vol. 9, No. 7, pp. 4328–4332, Jul. 2009.